BIOCHEMISTRY
including biophysical chemistry & molecular biology

Article

pubs.acs.org/biochemistry

Molecular Crowding Favors Reactivity of a Human Ribozyme Under Physiological Ionic Conditions

Christopher A. Strulson,[†,‡] Neela H. Yennawar,[§] Robert P. Rambo,[∥] and Philip C. Bevilacqua*[,†,‡]

[†]Department of Chemistry, The Pennsylvania State University, University Park, Pennsylvania 16802, United States
[‡]Center for RNA Molecular Biology, The Pennsylvania State University, University Park, Pennsylvania 16802, United States
[§]Huck Institutes of the Life Sciences, The Pennsylvania State University, University Park, Pennsylvania 16802, United States
[∥]Physical Biosciences Division, Lawrence Berkeley National Laboratory, Berkeley, California 94720, United States

Supporting Information

ABSTRACT: In an effort to relate RNA folding to function under cellular-like conditions, we monitored the self-cleavage reaction of the human hepatitis delta virus-like *CPEB3* ribozyme in the background of physiological ionic concentrations and various crowding and cosolute agents. We found that at physiological free Mg^{2+} concentrations (~0.1−0.5 mM), both crowders and cosolutes stimulate the rate of self-cleavage, up to ~6-fold, but that in 10 mM Mg^{2+} (conditions widely used for *in vitro* ribozyme studies) these same additives have virtually no effect on the self-cleavage rate. We further observe a dependence of the self-cleavage rate on crowder size, wherein the level of rate stimulation is diminished for crowders larger than the size of the unfolded RNA. Monitoring effects of crowding and cosolute agents on rates in biological amounts of urea revealed additive-promoted increases at both low and high Mg^{2+} concentrations, with a maximal stimulation of more than 10-fold and a rescue of the rate to its urea-free values. Small-angle X-ray scattering experiments reveal a structural basis for this stimulation in that higher-molecular weight crowding agents favor a more compact form of the ribozyme in 0.5 mM Mg^{2+} that is essentially equivalent to the form under standard ribozyme conditions of 10 mM Mg^{2+} without a crowder. This finding suggests that at least a portion of the rate enhancement arises from favoring the native RNA tertiary structure. We conclude that cellular-like crowding supports ribozyme reactivity by favoring a compact form of the ribozyme, but only under physiological ionic and cosolute conditions.

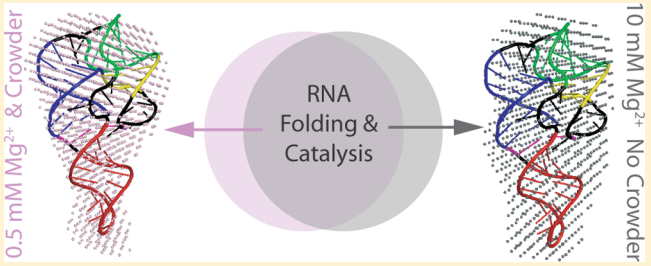

An overarching question in biological catalysis is whether and how cellular conditions act to facilitate function. Two key features of cells that differ from those of a dilute solution are compartmentalization of biomolecules and the presence of molecular crowding and cosolute agents. We recently demonstrated that compartmentalization of RNA in aqueous phase compartments can improve ribozyme catalysis by nearly 100-fold.[1] However, the extent to which molecular crowding and cosolutes affect catalysis remains unclear.

Up to 20−30% of the cellular volume in eukaryotic and prokaryotic cells is occupied by biopolymers, which provide crowded conditions that can affect RNA structure and function.[2−6] These high-molecular weight crowding agents exclude volume, alter solvent properties, and in some cases interact weakly with nucleic acids. In addition, low-molecular weight cosolutes such as NTPs,[7] amino acids,[8] and metabolites[9] are present in the cell at concentrations of tens of millimolar. These species can have strong interactions with nucleic acids as well as alter solvent properties.[10−13] Molecular crowders profoundly alter the thermodynamic and kinetic properties of biological macromolecules.[2] For example, physiological reaction rates and equilibria can differ from those in dilute buffers by orders of magnitude.[3]

Studies analyzing proteins revealed that protein stability, association rates, secondary structure folding, compaction, and function can be substantially impacted in the presence of macromolecular crowders.[10,14,15] For instance, kinetic studies of the monomeric protein enzyme EntC revealed that macromolecular crowders increase enzymatic activity through potential conformational and structural changes.[16] Futhermore, protein folding studies of ribonuclease A uncovered that macromolecular crowding agents PEG20000 and Ficoll70 restore compaction of the native state in the presence of a chemical denaturant.[17] We note that effects in these cases are moderate, with only 1.2−2.5-fold effects on k_{cat}. The studies mentioned above provide significant insight into protein behavior under cellular conditions; however, parallel studies of RNA are much more limited.

Recently, several studies of ribozyme folding and catalysis in the presence of crowder and cosolute additives have been conducted.[4−6,18,19] Such additives include higher-molecular

Received: June 24, 2013
Revised: October 7, 2013
Published: November 4, 2013

dx.doi.org/10.1021/bi400816s | *Biochemistry* 2013, 52, 8187−8197

weight polymers such as PEG1000, PEG8000, Dextran10, and Dextran70, which have average molecular weights of 1, 8, 10, and 70 kDa, respectively, and serve as crowders, as well as lower-molecular weight species such as urea, proline, betaine, sugars, glycerol, and PEG200, which serve as cosolutes or osmolytes.[20,21] While the studies mentioned above have provided insight into RNA function, thermodynamics, and compaction in the presence of such cellular additives, no study to date has linked ribozyme catalysis to molecular structure under cellular-like conditions, nor has a human ribozyme been examined.

An attractive RNA for studying the effects of crowding on catalysis is the self-cleaving human HDV-like *CPEB3* ribozyme. This ribozyme is structurally similar to the HDV ribozyme, with a double-pseudoknotted structure with five pairings. However, a few differences are found between these two RNAs.[22] One distinction is that the *CPEB3* ribozyme contains a weakened P1.1 pairing that is comprised of just a single GC Watson–Crick base pair (Figure 1), as opposed to the two GC base pairs

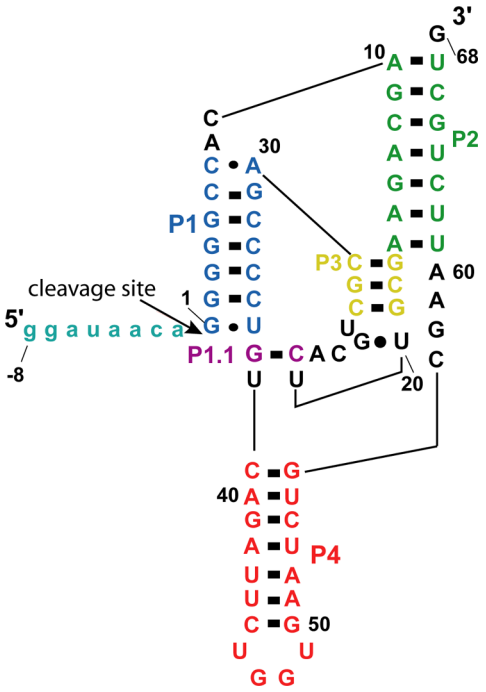

Figure 1. Secondary structure of the wild-type (WT) *CPEB3* ribozyme. The pairings (P1–P4 and P1.1) of the ribozyme are colored blue, green, yellow, orange, and purple, respectively. Shown is precursor −8/68 WT human RNA, where nucleotides upstream of the cleavage site (−8/−1) are colored teal.

found in the HDV ribozyme.[22] We previously demonstrated that this weakened P1.1 pairing leads the *CPEB3* ribozyme to switch between the native state and a misfolded state incapable of catalysis.[23] In addition, several residues in the *CPEB3* ribozyme are single-stranded in the native state and so are likely mobile (Figure 1). Because macromolecular crowding generally shifts the equilibrium of large biomolecules toward compact structures, we reasoned that the *CPEB3* ribozyme might show improved kinetic activity in the presence of crowding agents.

Herein, we demonstrate that crowding and cosolute agents stimulate human ribozyme kinetics at physiological magnesium concentrations, but not high magnesium concentrations. In addition, we show that crowding and cosolute agents protect as well as refold the RNA in the presence of a denaturant. SAXS studies reveal that at physiological magnesium concentrations higher-molecular weight crowders act to appreciably compact the RNA, while a stabilizing cosolute has relatively little effect on the global structure.

MATERIALS AND METHODS

RNA Preparation. Following are the sequences of the *CPEB3* wild-type (WT) and C-2A mutant precleaved ribozymes used in this study. The sequence upstream of the cleavage site is shown in lowercase, and the mutated nucleotide (nt) is shown in bold: WT (76 nt), 5′-ggauaacaGGGGGCCACAGCAGAAGCGUUCACGUCGCAGCCCCUGUCAGAUUCUGGUGAAUCUGCGAAUUCUGCUG; C-2A (76 nt), 5′-ggauaaaaGGGGGCCACAGCAGAAGCGUUCACGUCGCAGCCCCUGUCAGAUUCUGGUGAAUCUGCGAAUUCUGCUG. For RNA transcribed for kinetics studies, the following procedure was used to isolate full length precleaved (−8/68) RNA. Both the WT and the C-2A mutant were transcribed from linearized plasmid (*Bsa*I-digested) DNA using a modified transcription procedure to limit self-cleavage during the transcription process, and this procedure was followed without modification.[23] Specifically, to prepare uncleaved RNA for kinetic reactions, transcriptions were performed at a reduced temperature of 23 °C and for only 2 h. The WT and C-2A *CPEB3* ribozymes were transcribed in the presence of [γ-^{32}P]GTP to 5′-end label the RNA. This procedure eliminates the need for dephosphorylation and end labeling steps, which lead to extensive self-cleavage. Labeled full length precleaved RNA was gel purified and precipitated for use in kinetic experiments.

The following procedure was used to isolate large amounts of fully cleaved (1/68) RNA for SAXS experiments. The WT *CPEB3* RNA was transcribed from linearized plasmid DNA at 37 °C for 4 h, a higher temperature and a longer time to promote both enhanced transcription yields and extents of cleavage during transcription. At this point, negligible full length RNA was present, as most had been cleaved during transcription. The cleaved ribozyme was purified by denaturing polyacrylamide gel electrophoresis (PAGE) and precipitated. RNA was then buffer exchanged using an Amicon Ultra centrifugal filter (molecular weight cutoff of 3 kDa) in either 25 mM HEPES (pH 8), 100 mM KCl, and 0.5 mM $MgCl_2$ or 25 mM HEPES (pH 8), 100 mM KCl, and 10 mM $MgCl_2$. PEG200 and PEG8000 stock solutions were prepared in the same buffer so that the buffer and salt concentrations were not diluted.

Cleavage Experiments and Data Fitting. For each reaction, ∼2 nM of [γ-^{32}P]GTP end-labeled RNA was renatured at 90 °C for 3 min in 1× TE and allowed to cool to room temperature for 10 min. Reaction buffer consisted of 25 mM HEPES (pH 8), 100 mM KCl, and varying Mg^{2+} concentrations. Buffers were prepared using ultrapurified deionized water and filtered using 0.5 μm filters. Crowding and cosolute agents were added before Mg^{2+} unless otherwise noted. PEG200, Dextran10, Dextran40, Dextran70, and Ficoll70 were from Sigma-Aldrich (St. Louis, MO), and PEG8000 (average molecular weight of 8 kDa) was from Research Organics (Cleveland, OH) and used within the first 3–4 months of being opened without further purification. The concentration of additives is in percent (w/v) unless otherwise noted. Reactions were initiated by the addition of Mg^{2+}. Time points were removed and added to an equal volume of 95%

dx.doi.org/10.1021/bi400816s | *Biochemistry* 2013, 52, 8187–8197

formamide loading buffer with 0.1 M EDTA and immediately placed on dry ice. Aliquots were fractionated on a denaturing 10% PAGE gel and dried. Gels were visualized using a PhosphorImager and analyzed using ImageQuant (Molecular Dynamics).

Plots of product fraction versus time were generated and fit to a single-exponential equation (eq 1),

$$f_c = A + Be^{-k_{obs}t} \quad (1)$$

where f_c is the fraction of precursor substrate cleaved, k_{obs} is the observed first-order rate constant, t is time, A is the fraction of substrate cleaved at completion, and $-B$ is the amplitude of the observable phase. All kinetic parameters were obtained using least-squares fitting by KaleidaGraph (Synergy Software). Kinetic traces that gave ≤20% reaction after 2 h were fit to a linear equation. Each data point was the average of at least two trials ± the standard deviation of the experiments. In plots that contain "fold stimulation", the error on the plot is propagated from the errors in the compared conditions.

Model of the Human *CPEB3* Ribozyme. The crystal structure of the HDV ribozyme deposited in the Protein Data Bank (entry 3NKB) was used as the starting point for building a model of the human *CPEB3* ribozyme using COOT.[24] The bases were mutated from the HDV to the human *CPEB3* ribozyme sequence, and base pairing in the P1, P1.1, and P2–P4 was maintained. Of special note, the GC base pair at the base of P1.1 in the HDV ribozyme was changed to a U·U wobble pair, the "GCA" stretch under P1.1 was deleted, and P4 was stacked onto the U·U wobble pair. Other key interactions were maintained, including the G·U wobble pair at the base of P1, the reverse G·U wobble pair at the base of P3, the stacking of P1, P1.1, and P4, the stacking of P2 and P3, and the interaction of N3 of C57 with the 5′-OH group of G1. The UGGU loop modeled at the base of P4 was identified using COSSMOS.[25] The resulting coordinates were subjected to energy minimization using the online YASARA server.[26] The energy-minimized model was rechecked for known tertiary interactions and used as the monomer model for fitting with the SAXS data.

SAXS Data Collection. The cleaved (1/68) *CPEB3* ribozyme was prepared as described above and used for SAXS analysis. To test for aggregation, three concentrations of the RNA (0.2, 0.4, and 0.6 mg/mL) were prepared at both 0.5 and 10 mM Mg^{2+}, with and without 20% PEG200 and PEG8000. Dextran was not used because it is known to be a strong scatterer. RNA was renatured at 55 °C for 3 min and allowed to cool to room temperature for 10 min followed by the addition of the cosolute (the sample with buffer alone was also renatured). The RNA solution was centrifuged at 14K rpm for 10 min prior to data collection to degas and remove any dust. Initial SAXS data were collected on CHESS beamline F2 at 9.881 keV (1.2563 Å, the tantalum edge). The X-ray beam was collimated to a 250 μm × 250 μm area and centered on a 2 mm diameter vertical quartz capillary tube with 10 μm thick walls (Hampton Research, Aliso Viejo, CA). To eliminate air scatter, the capillary tube and full X-ray flight path, including the beam-stop, were kept *in vacuo*. Sample plugs of approximately 25–30 μL were delivered from a 96-well plate to the capillary using a Hudson SOLO single-channel pipetting robot (Hudson Robotics Inc., Springfield, NJ). A computer-controlled syringe pump (Aurora Biomed, Vancouver, BC) was used to keep the sample liquid oscillating in the X-ray beam to reduce radiation damage. Fifteen scattering images were collected on a Quantum 1 CCD detector (Area Detector Systems Corp., Poway, CA) with sequential 180 s exposures to assess possible radiation damage. No radiation damage was detected in the RNA solutions, as multiple scans of the same sample provided similar scattering. The sample-to-detector distance was calibrated using silver behenate powder (The Gem Dugout, State College, PA).

Solution scattering images were reduced to profiles and buffer-subtracted using BioXTAS RAW.[27] Scaling of the scattering curves in the presence of PEG200 and PEG8000 was conducted because macromolecule contrast decreases in the presence of PEG.[28] Therefore, scattering profiles obtained in the presence of PEG200 and PEG8000 were scaled to buffer-only profiles. While the useful q space range of $4\pi \sin(\theta)/\lambda$ (with 2θ being the scattering angle) was determined on a case-by-case basis using the Guinier plot as a guide, it was generally the case that q_{min} equaled 0.02 $Å^{-1}$ and q_{max} equaled 0.25 $Å^{-1}$.

SAXS data at 10 mM Mg^{2+} in the absence of additive were contaminated by residual aggregates; therefore, for these samples we performed size-exclusion chromatography (SEC) of annealed RNA samples immediately prior to SAXS at the SIBYLS beamline.[29,30] Briefly, RNA samples were annealed at either 0.1 or 1 mg/mL as described above in buffer containing 10 mM $MgCl_2$ and concentrated to 5 mg/mL. Then, 50 μL samples were injected onto a Shodex KW402.4 4.2 mL column in buffer pre-equilibrated with 25 mM HEPES (pH 8), 100 mM KCl, and 10 mM $MgCl_2$, and a peak fraction corresponding to ∼1 mg/mL (40–60 μL) was taken for SAXS analysis as previously described[30] with two exposures at 0.5 and 1 s.

SAXS Data Analysis. SAXS data were initially collected on RNA solutions at the three different concentrations listed above to determine the extent of interparticle interference and concentration effects. Six solution conditions were tested: buffer alone, 20% PEG200, and 20% PEG8000 each in 0.5 and 10 mM Mg^{2+}. For SAXS data analysis, scattering data at 0.6 mg/mL RNA were used for generation of the plots described below in 0.5 mM Mg^{2+} because the sample was monodisperse and this concentration showed an increased signal:noise ratio. In 10 mM Mg^{2+}, data collected in the presence of PEG8000 were at 0.4 mg/mL RNA, while data in the absence of a crowder were collected subsequent to SEC as described above. The radius of gyration (R_g) was calculated using both the method of Guinier[31] and the inverse Fourier transform (IFT) method as implemented in GNOM (Table 1).[32] In the Guinier method, linear fitting was performed on data having a qR_g range of <1.3. Interactive fitting was performed using BioXTAS RAW.[27] The maximal diameter of the RNA (D_{max}) was determined by plotting the total estimate scores[33] and χ^2 on a range of D_{max} values using the RunGnomRun script.[34] In addition, dimensionless Kratky plots were generated for 0.5 mM Mg^{2+}.[35]

The experimental SAXS data were compared to the model of the human *CPEB3* ribozyme using the FoXS server.[36,37] The program fits a given atomic structure to an experimental scattering curve optimizing particle hydration. Shape reconstructions were performed with 10 independent DAMMIF calculations[38] using the ATSAS server with no symmetry conditions. The server outputs a consensus reconstruction using DAMAVER,[39] and the most probable model from DAMFILT is presented. Superposition of the DAMFILT model with the RNA model was done using SUPCOMB20, which was also used to calculate the rmsd and average excluded

volume.[40] The superposed SAXS reconstruction envelopes and RNA models were visualized using PYMOL (The PyMOL Molecular Graphics System, version 1.3, Schrödinger, LLC).

RESULTS

Ribozyme Reactivity Is Favored by Crowding and Cosolute Agents at Low but Not High Magnesium Concentrations. We began by exploring the effects of the cosolute PEG200 and the higher-molecular weight crowding agents PEG8000 and Dextran10 on *CPEB3* ribozyme function. All studies were conducted on a one-piece form of the ribozyme, rather than a two-piece substrate−enzyme form, because the one-piece is the form it assumes in nature and is most likely to report biologically relevant folding. These polymers were chosen because their impacts on nucleic acid folding have been described in the literature: PEG200 is a cosolute that preferentially interacts with nucleic acids[21,41] and changes the dielectric of the solution,[13] and PEG8000 and Dextran10 act as macromolecular crowding agents.[5,41] The effects of these additives on *CPEB3* ribozyme activity were studied herein at both *in vivo*-like free Mg^{2+} concentrations (0.1 and 0.5 mM) and standard *in vitro* Mg^{2+} concentrations (10 mM), both in the background of *in vivo*-like 100 mM KCl. Concentrations of free Mg^{2+} in eukaryotic cells have been estimated to range between 0.2 and 1 mM.[42−45]

In the presence of 10 mM Mg^{2+}, the crowding agents and cosolute had essentially no effect on the rate (Figure 2); for instance, the k_{obs} for self-cleavage was 0.040 ± 0.006 min^{-1} without additives and 0.036 ± 0.006, 0.044 ± 0.008, and 0.036 ± 0.007 min^{-1} in the presence of 30% (w/v) PEG200, 30% (w/v) PEG8000, and 30% (w/v) Dextran10, respectively (Table S1 of the Supporting Information). The lack of rate enhancement at high Mg^{2+} concentrations suggests that the ribozyme may already be well-folded under standard *in vitro* conditions, which is not surprising because these nonphysiological Mg^{2+} conditions (high concentrations) have been developed in the field for their ability to strongly promote RNA folding.

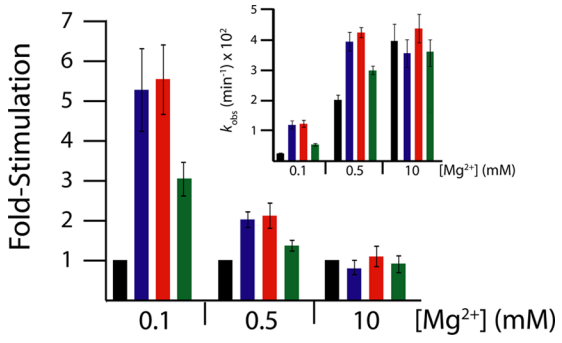

Figure 2. Stimulation of WT *CPEB3* ribozyme kinetics by crowding and cosolute agents occurs at physiological magnesium concentrations. The main plot displays relative rate enhancement reported as "fold-stimulation" by comparing the rate with the additive to the rate with buffer only (black) for each magnesium concentration, where PEG200 (blue), PEG8000 (red), and Dextran10 (green) were present at a concentration of 30% (w/v). The inset shows the raw self-cleavage rates of the WT *CPEB3* ribozyme for the conditions described above. Observed cleavage rate constants in 0.5 and 10 mM Mg^{2+} are provided in Table S1 of the Supporting Information.

In contrast to strongly folding conditions, crowding and cosolute agents do promote the rate of the reaction under weakly folding ionic conditions of 0.5 mM Mg^{2+} (Figure 2). In particular, the rate of ribozyme self-cleavage is stimulated ∼1.5−2.3-fold by the presence of PEG200, PEG8000, and Dextran10 (Table S1 of the Supporting Information). Moreover, the rates in 0.5 mM Mg^{2+} with additives are identical, within error, to the rates in 10 mM Mg^{2+}. This indicates that PEG200, PEG8000, and Dextran10 lessen the Mg^{2+} requirement for the reaction, leading to maximal rates at biological Mg^{2+} concentrations.

To see if rate enhancement by additives could be further enhanced, we determined the effect of these additives in the presence of just 0.1 mM Mg^{2+}, which is close to the lower estimates for physiological free Mg^{2+} concentrations.[42−45] Under these conditions, the rate increased from 0.0021 ± 0.0003 min^{-1} in the absence of additives to 0.011 ± 0.002, 0.012 ± 0.001, and 0.007 ± 0.001 min^{-1} in the presence of PEG200, PEG8000, and Dextran10, respectively, leading to overall increases in rate of 3−6-fold in the presence of an additive (Figure 2).[a] It is interesting to note that these effects are substantially larger than those seen for k_{cat} in the protein enzyme examples mentioned above, which were 1.2−2.5-fold.[16,17]

Next, the dependence of the rate on the concentrations of the crowding and cosolute agents was explored over the range of 10−40% additive. As shown in Figure S1 of the Supporting Information, under conditions of 0.5 mM Mg^{2+} the stimulation of cleavage was maximal at ∼30% PEG200, 30% PEG8000, and 30% Dextran10, which remarkably is in the realm of biological crowding.[3] Higher concentrations of these additives led to either no further stimulation or to inhibition. In an effort to explore the role of additives in the reaction, kinetic assays were also performed in 30% PEG200, 30% PEG8000, and 30% Dextran10 but without added Mg^{2+}. As expected, no cleavage was observed for any of these conditions (data not shown), consistent with a requirement for a catalytic Mg^{2+} ion in the reaction[22,46] and confirming that the additive does not act as a Mg^{2+} surrogate or contain significant amounts of contaminating cations.

The effects of higher-molecular weight crowders were also tested at the various magnesium concentrations. Dextran40, Dextran70, and Ficoll70, which have average molecular weights of 40, 70, and 70 kDa, respectively, were used to determine the effects of higher-molecular weight crowders on *CPEB3* function. In the presence of 10 mM Mg^{2+}, the higher-molecular weight crowding agents had essentially no effect on the rate (Figure S2 of the Supporting Information). For instance, the k_{obs} for self-cleavage was 0.040 ± 0.006 min^{-1} without additives and 0.051 ± 0.006, 0.044 ± 0.008, and 0.047 ± 0.007 min^{-1} in the presence of 30% (w/v) Dextran40, 30% (w/v) Dextran70, and 30% (w/v) Ficoll70, respectively, consistent with the results described above for crowders PEG8000 and Dextran10 in 10 mM Mg^{2+}. However, in 0.1 and 0.5 mM Mg^{2+}, where substantial increases in cleavage rate were achieved by adding PEG8000 and Dextran10 to the cleavage reaction mixture, the higher-molecular weight crowders also had little or no stimulatory effect. For example, Dextran40 led to ∼2.5- and 2-fold increases in the extent of cleavage versus that of buffer alone in 0.1 and 0.5 mM Mg^{2+}, respectively, while Dextran70 and Ficoll70 led to minimal stimulatory effects of up to only 1.3-fold in 0.1 and 0.5 mM Mg^{2+} (Figure S2 of the Supporting Information). These data reveal a clear size dependence of the stimulatory effect gained by the presence of macromolecular crowders. Given that the RNA studied here has a molecular

weight for the pre-cleaved form of ~25 kDa, this trend is in agreement with theoretical predictions, where crowders larger than the size of the unfolded RNA are predicted to have diminishing effects on RNA stability.[47]

Because both cosolutes and moderate molecular weight crowders stimulated the cleavage reaction, we probed whether local magnesium concentrations were being influenced by interactions between the additives and magnesium. Vapor-pressure osmometry was used to determine the activity of water in the presence of Mg^{2+}, PEG200, PEG8000, and Dextran10. The activity of water was determined as a function of 0−10 mmol/kg Mg^{2+} parametric in 10 and 20% (w/v) additives (Figure S3 of the Supporting Information). It was found that the additives and magnesium affect the activity of water independently, supporting the notion that the additives do not significantly influence the free Mg^{2+} concentration.

Ribozyme Reactivity Is Favored by Crowding and Cosolute Agents at Low and High Magnesium Concentrations in the Presence of Urea. We reasoned that because the synthetic polymers rescued ribozyme activity under only weakly folding Mg^{2+} concentrations (0.1 and 0.5 mM Mg^{2+}), the polymers may be acting as renaturants of RNA folding. To test this idea, we assessed whether these polymers could enhance ribozyme activity in the presence of a denaturant. Urea was chosen as the denaturant for several reasons. First, it is a biologically relevant denaturant, as it can reach concentrations up to 0.6 *m* in certain plant and bacterial species[48] and 5 *m* in kidney cells.[49] Second, urea is known to generally denature RNA secondary and tertiary structure.[20,50,51] Indeed, we found self-cleavage of the *CPEB3* ribozyme to be sensitive to biological concentrations of urea (Figure 3 and Figure S4 of the Supporting Information). For example, in a background of 0.5 mM Mg^{2+}, 0.5 M urea led to ~2-fold slower cleavage, while 2.5 M urea produced 11-fold slower cleavage. In the background of 10 mM Mg^{2+}, urea also slowed the rate, albeit with weaker, 2-fold effects (Figure 4).

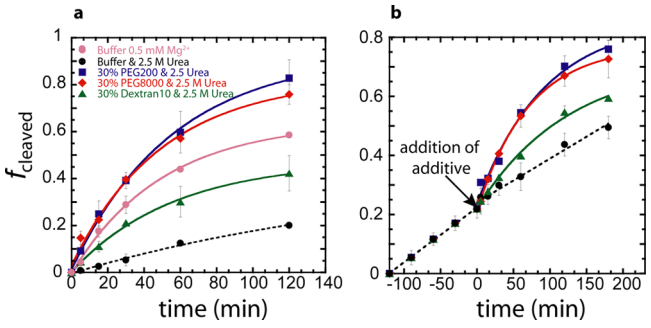

Figure 3. Self-cleavage of the WT *CPEB3* ribozyme in 0.5 mM Mg^{2+} and 2.5 M urea with crowding and cosolute agents. PEG200, PEG8000, and Dextan10 were present at final concentrations 30% (w/v). (a) Crowding and cosolute additives are present in the reaction solution prior to simultaneous addition of urea and Mg^{2+}. (b) Crowding and cosolute additives were added 120 min after addition of urea and Mg^{2+}, keeping the urea and Mg^{2+} concentration constant throughout.

To assess whether crowding and cosolute agents could act as a renaturant and to improve our understanding of the roles crowders and cosolutes might play *in vivo*, we tested whether part or all of the 11-fold loss of *CPEB3* cleavage activity in 2.5 M urea and 0.5 mM Mg^{2+} could be rescued by crowding and cosolute additives. Initially, the additive was present before the urea and Mg^{2+}. As shown in Figure 3a, each additive protected the ribozyme from the inhibitory effects of urea to some degree; for instance, the cleavage rate in 0.5 mM Mg^{2+} and 2.5 M urea was 0.0017 ± 0.0005 min^{-1} but increased more than 10-fold to 0.018 ± 0.001, 0.020 ± 0.003, and 0.018 ± 0.002 min^{-1} in the presence of PEG200, PEG8000, and Dextran10, respectively (Table S1 of the Supporting Information and Figure 4). These rescued values are close to the urea-free rate constant of 0.019 min^{-1} in 0.5 mM Mg^{2+}, indicating that the additives fully rescue the rate. In 2.5 M urea and 10 mM Mg^{2+}, the additives also stimulated the rate back to urea-free values (Figure 4).

We next investigated whether the cosolute and crowding additives could refold the RNA when the destabilizing osmolyte was already present in the solution. In this case, the reaction was initiated with 0.5 mM Mg^{2+} in the presence of 2.5 M urea, and after 2 h, the crowding or cosolute agent was added, while a constant ionic strength was maintained (Figure 3b). Remarkably, crowding and cosolute agents restored catalysis to the levels observed for the first order of addition without any detectable lag. This finding demonstrates that at biological magnesium concentrations, crowding and cosolute agents can overcome the inhibitory effects of destabilizing osmolytes, effectively acting as nonspecific chaperones to promote RNA folding.

To establish the degree to which crowding and cosolute agents may aid native RNA folding at lower urea concentrations, cleavage rates were measured in the background of just 0.5 M urea in both 0.5 and 10 mM Mg^{2+}. In 10 mM Mg^{2+}, 0.5 M urea had an approximately 2-fold inhibitory effect on the cleavage rate, and crowding and cosolute agents rescued this loss (Figure 4). In 0.5 mM Mg^{2+}, 0.5 M urea also had an ~2-

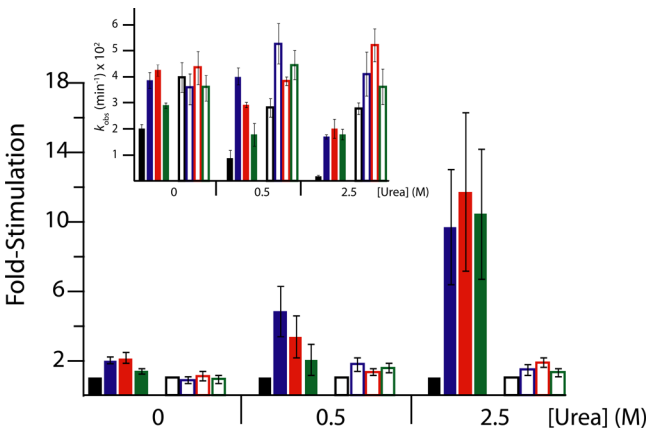

Figure 4. Stimulation of WT *CPEB3* ribozyme kinetics by crowding and cosolute agents at various concentrations of magnesium and urea. The main plot displays the relative rate enhancement reported as fold-stimulation by comparing the rate with the additive to the rate with buffer only (black) for each Mg^{2+} concentration, where PEG200 (blue), PEG8000 (red), and Dextran10 (green) are present at concentrations of 30% (w/v). Biological free Mg^{2+} (0.5 mM Mg^{2+}, filled bars) and standard Mg^{2+} (10 mM Mg^{2+}, empty bars) were both used to evaluate ribozyme function under these conditions. Three urea concentrations were chosen to represent varying conditions: 0 M urea (highly folded), 0.5 M urea (denaturing), and 2.5 M urea (highly denaturing). The inset shows the raw self-cleavage rates for the WT *CPEB3* ribozyme for the conditions described above. Observed cleavage rate constants are listed in Table S1 of the Supporting Information.

dx.doi.org/10.1021/bi400816s | *Biochemistry* 2013, 52, 8187−8197

fold inhibitory effect on cleavage (Figure 4), but crowding and cosolute agents had an up to ~5-fold stimulatory effect, restoring the rate to its values in the presence of these additives without urea (Figure 4).

We probed whether local urea concentrations were being influenced by interactions with additives using vapor-pressure osmometry. The activity of water was determined as a function of 0–2 mol/kg urea in the presence of 10 and 20% (w/v) PEG8000 or 10 and 20% (w/v) Dextran10 (Figure S5 of the Supporting Information). PEG200 was not used because at these urea concentrations the vapor-pressure readings were out of the range of linearity for the instrument. We found that the additives and urea affect the activity of water in a largely independent manner.

Reactivity of the Fast-Reacting C-2A Mutant Is Also Favored by Crowding and Cosolute Agents. As described above, crowding and cosolute agents stimulated wild-type *CPEB3* ribozyme self-cleavage both with and without urea (Figure 4). To test the generality of this trend, a faster-cleaving mutant of the *CPEB3* ribozyme termed C-2A was transcribed, and cleavage assays were conducted under urea, Mg^{2+}, and additive conditions identical to those described above. The C-2A change functions to destabilize a misfold termed "Alt P1" between the ribozyme sequence and nucleotides upstream of the cleavage site,[23] which is depicted in Scheme 1.

Scheme 1

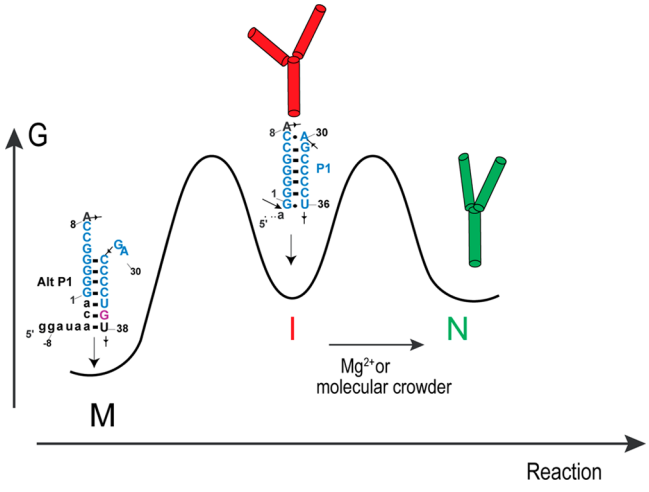

Despite the absence of the stable Alt P1 misfold, the C-2A ribozyme exhibited kinetic trends similar to those of the WT *CPEB3* ribozyme at various Mg^{2+} and urea concentrations upon the addition of crowding and cosolute agents (Figure 5). For instance, in 0.5 mM Mg^{2+}, 0.5 M urea again inhibited cleavage 2-fold, and additives restored the rate to the values found in the presence of additives without urea. The similarity of the trends demonstrates that the stimulatory effects of the additives reflect features of the equilibrium between the intermediate and native state rather than the need to escape an alternative pairing.

SAXS Studies Reveal Compaction in the Presence of a Crowder. In an effort to relate the rate stimulatory effects of crowding and cosolute agents mentioned above to RNA structure, small-angle X-ray scattering (SAXS) experiments were performed. SAXS was chosen for this portion of the study because it provides information about the global structure of RNA in the presence of the polymers.[4] The cleaved *CPEB3* ribozyme (1/68) was used in the SAXS experiments. The

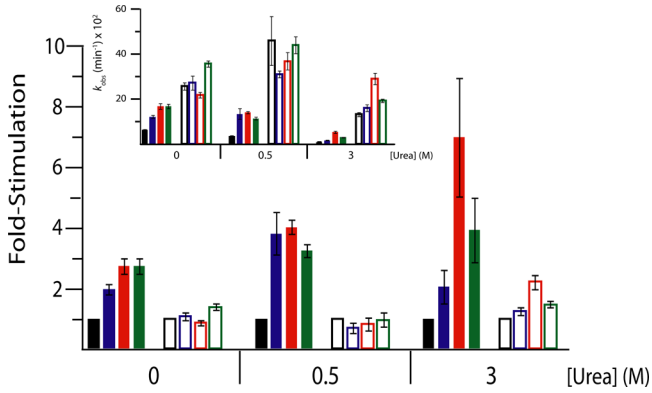

Figure 5. Stimulation of C-2A *CPEB3* ribozyme kinetics by crowding and cosolute agents at various concentrations of magnesium and urea. The main plot displays the relative rate enhancement reported as fold-stimulation by comparing the rate with the additive (colored as described below) to the rate with buffer only (black) for each Mg^{2+} concentration, where PEG200 (blue), PEG8000 (red), and Dextran10 (green) are present at concentrations of 20, 40, and 40%, respectively. Biological free Mg^{2+} (0.5 mM Mg^{2+}, filled bars) and standard Mg^{2+} (10 mM Mg^{2+}, empty bars) were both used to evaluate the difference between ribozyme function under these conditions. The three urea concentrations were chosen as described in the legend of Figure 4. The inset shows the raw self-cleavage rates for the C-2A *CPEB3* ribozyme for the conditions described above. Observed cleavage rate values are listed in Table S1 of the Supporting Information.

cleaved form is relevant to the reaction, as previous studies of the structurally similar HDV ribozyme have demonstrated that the cleaved form has a fold very similar to that of the precleaved form and captures many of the critical catalytic interactions.[46,52]

We provide the scattering profiles of the *CPEB3* ribozyme in 0.5 and 10 mM Mg^{2+}, both in 100 mM KCl in Figure 6a and Figure S6 of the Supporting Information, respectively. Data were collected under three different conditions in 0.5 mM Mg^{2+}: buffer alone, 20% PEG200, and 20% PEG8000. In 10 mM Mg^{2+}, data were collected for buffer alone and 20% PEG8000. These data reveal a standard decay of intensity with q, with similar but somewhat different curves for each condition. Also provided in these figures as insets are Guinier analyses, which show linearity to small q. The Guinier analyses allow us to obtain radii of gyration (R_g) under these various conditions, which are listed Table 1.

We assessed R_g values for the cleaved *CPEB3* ribozyme in both 0.5 and 10 mM Mg^{2+}. The R_g value from Guinier analysis in 0.5 mM Mg^{2+} and buffer is 23.6 Å. Upon addition of PEG200 to a concentration of 20%, the R_g value increased to 26.1 Å, suggesting that PEG200 does not compact the RNA and in fact may expand it. In contrast, addition of PEG8000 to a concentration of 20% decreased the R_g to 21.3 Å, which suggests that the increase in rate in PEG8000 observed above may arise from compaction of the fold. This is further bolstered by agreement with an R_g of 20.4 Å from our model of the native state (described below).

We anticipated that as the Mg^{2+} concentration increased, a compaction of the RNA would occur, as observed by Woodson and colleagues for a group I ribozyme.[4] However, we found that the SAXS-derived R_g values determined in buffer without an additive increased from 23.6 to 28.5 Å as the Mg^{2+} concentration was increased from 0.5 to 10 mM. These data suggest that aggregation of the sample may occur in 10 mM

dx.doi.org/10.1021/bi400816s | *Biochemistry* 2013, 52, 8187–8197

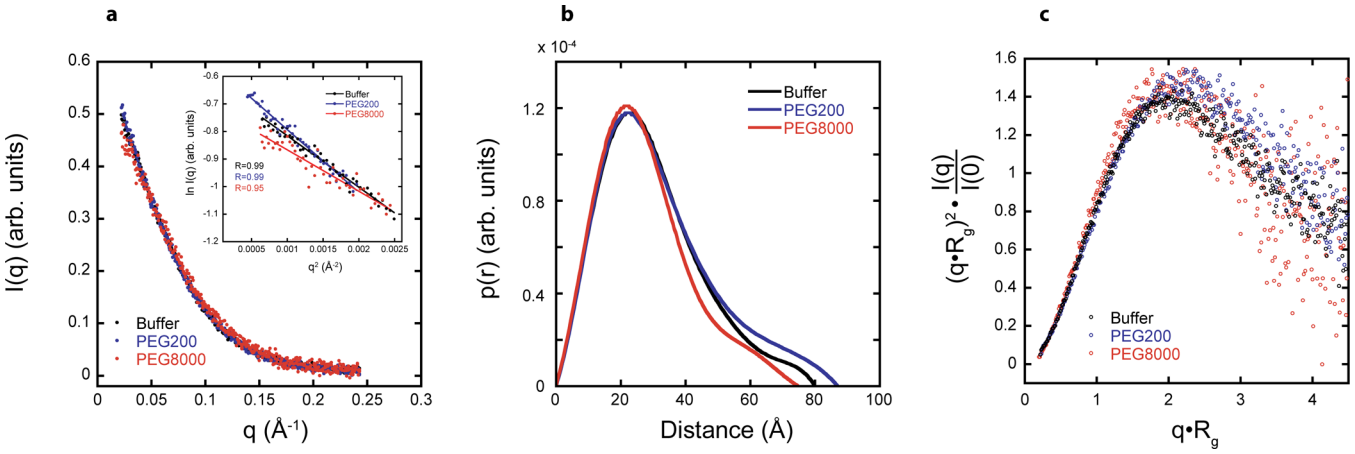

Figure 6. SAXS scattering profiles, $p(r)$ plots, and Kratky plots in 0.5 mM Mg^{2+} help describe the global folds. For all panels, plots are for RNA in buffer (black), buffer with 20% PEG200 (blue), and buffer with 20% PEG8000 (red). (a) Scattering profile. RNA scattering profiles in the presence of PEG200 and PEG8000 are normalized to RNA scattering profiles in buffer alone to account for differences in contrast. R_g was determined from data in the Guinier regime ($qR_g < 1.3$) (inset), and R_g values are listed in Table 1. Linear behavior extending to low q values supports the absence of aggregation. (b) $p(r)$ plots. For PEG8000, the distribution is narrower and the peak is at smaller distance, which is reflected in a smaller R_g. (c) Dimensionless Kratky plots. These shapes are consistent with a folded native state and the absence of significant unstructured regions.

Table 1. SAXS-Determined R_g and D_{max} Values for the *CPEB3* Ribozyme with Crowding and Cosolute Agents[a]

	$R_{g(Guinier)}$ (Å)	$R_{g(GNOM)}$ (Å)	D_{max} (Å)	excluded volume (Å^3)
		0.5 mM Mg^{2+}		
buffer	23.6 ± 0.1	23.6 ± 0.4	80	44555
20% PEG200	26.1 ± 0.5	25.4 ± 0.5	87	45570
20% PEG8000	21.3 ± 0.1	21.8 ± 0.7	75	40544
		10 mM Mg^{2+}		
buffer	22.0 ± 0.6	22.6 ± 0.1	75	41280
20% PEG8000	19.9 ± 0.7	20.2 ± 0.8	67	30877

[a]The model of the *CPEB3* ribozyme gives an R_g of 20.4 Å and a D_{max} of 73.8 Å. The 0.5 mM Mg^{2+} data were recorded at an RNA concentration of 0.6 mg/mL, the 10 mM Mg^{2+} data in 20% PEG8000 at an RNA concentration of 0.4 mg/mL, and the 10 mM Mg^{2+} data in buffer alone at an RNA concentration of ∼1 mg/mL immediately following size-exclusion chromatography. SUPCOMB20 was used to calculate the rmsd and average excluded volume.[40]

Mg^{2+} but not 0.5 mM Mg^{2+}. Aggregation in 10 mM Mg^{2+} was also supported by dynamic light scattering (data not shown).

To provide an additional assay for aggregation, native gels were run using buffer conditions and RNA concentrations identical to those in the SAXS experiments at both 0.5 and 10 mM Mg^{2+}. Native gel data are provided in Figure S7 of the Supporting Information. A very low level of aggregation was present on native gels in 0.5 mM Mg^{2+} for 0.2, 0.4, or 0.6 mg/mL RNA. In contrast, appreciable aggregation was observed in native gels at 10 mM Mg^{2+} for all three concentrations of RNA, consistent with the larger R_g values from the SAXS experiments. Native gel lanes with trace RNA concentrations, similar to those used in kinetic experiments, showed virtually no aggregation at either Mg^{2+} concentration (Figure S7 of the Supporting Information).

Because aggregation of RNA was observed in samples with 10 mM Mg^{2+} and buffer alone, we used SEC to isolate a monomeric fraction for SAXS analysis. A sharp, fast mobility peak correlating to the monomeric RNA was collected and used for SAXS data collection. Analysis of this peak revealed an R_g of 22.0 Å, which shows compaction compared to the RNA in 0.5 mM Mg^{2+} in buffer alone (Table 1). Strikingly, the R_g of 22.0 Å for the RNA in 10 mM Mg^{2+} buffer alone is very similar to the R_g of 21.3 Å in 0.5 mM Mg^{2+} with 20% PEG8000.

Next, we conducted a GNOM analysis of the data. Both R_g and D_{max} values from GNOM analysis are listed in Table 1. We begin with analysis of 0.5 mM Mg^{2+} data. The R_g values from GNOM analysis are in excellent agreement with those from the Guinier analysis in 0.5 mM Mg^{2+}. The GNOM-generated $p(r)$ plots for 0.5 mM Mg^{2+} are provided in Figures 6b. For 0.5 mM Mg^{2+}, D_{max} values of 80, 87, and 75 Å were obtained in buffer, PEG200, and PEG8000, respectively. This trend in D_{max} values agrees well with the trend observed for the R_g values in 0.5 mM Mg^{2+}. Additionally, the shape of the distribution in 20% PEG8000 and 0.5 mM Mg^{2+} is somewhat narrower, and the maximum is at a slightly smaller distance than for PEG200 or buffer only (Figure 6b), which is reflected in the smaller R_g for PEG8000 (Table 1). Overall, these data support compaction of the ribozyme by high-molecular weight crowders in 0.5 mM Mg^{2+}.

The $p(r)$ plots for 10 mM Mg^{2+} were constructed in buffer only and 20% PEG8000 and are provided in Figure S6 of the Supporting Information. The R_g values from the GNOM analysis agree well with the R_g values obtained from the Guinier analysis for both the buffer alone and PEG8000 in 10 mM Mg^{2+}. In buffer alone, the D_{max} value was 75 Å, which is identical to that observed for the RNA in 0.5 mM Mg^{2+} and PEG8000. This mirrors the similarity in R_g values for these two conditions, presented above. Introduction of 20% PEG8000 into the background of 10 mM Mg^{2+} leads to further compaction, to a D_{max} value of 67 Å. Interestingly, this further compaction does not lead to an enhancement in catalysis, suggesting that it may occur outside the catalytic core (see Discussion).

Kratky plots can reveal information about the degree of folding of an RNA. For example, globular RNAs typically have Kratky plots shaped like an inverted parabola, while Kratky plots for partially unfolded RNAs do not return to baseline at large q values and can even drift upward or show a second feature.[53,54] Dimensionless Kratky plots for 0.5 mM Mg^{2+} are shown in Figure 6c. The Kratky plots in all conditions slope

dx.doi.org/10.1021/bi400816s | *Biochemistry* 2013, 52, 8187−8197

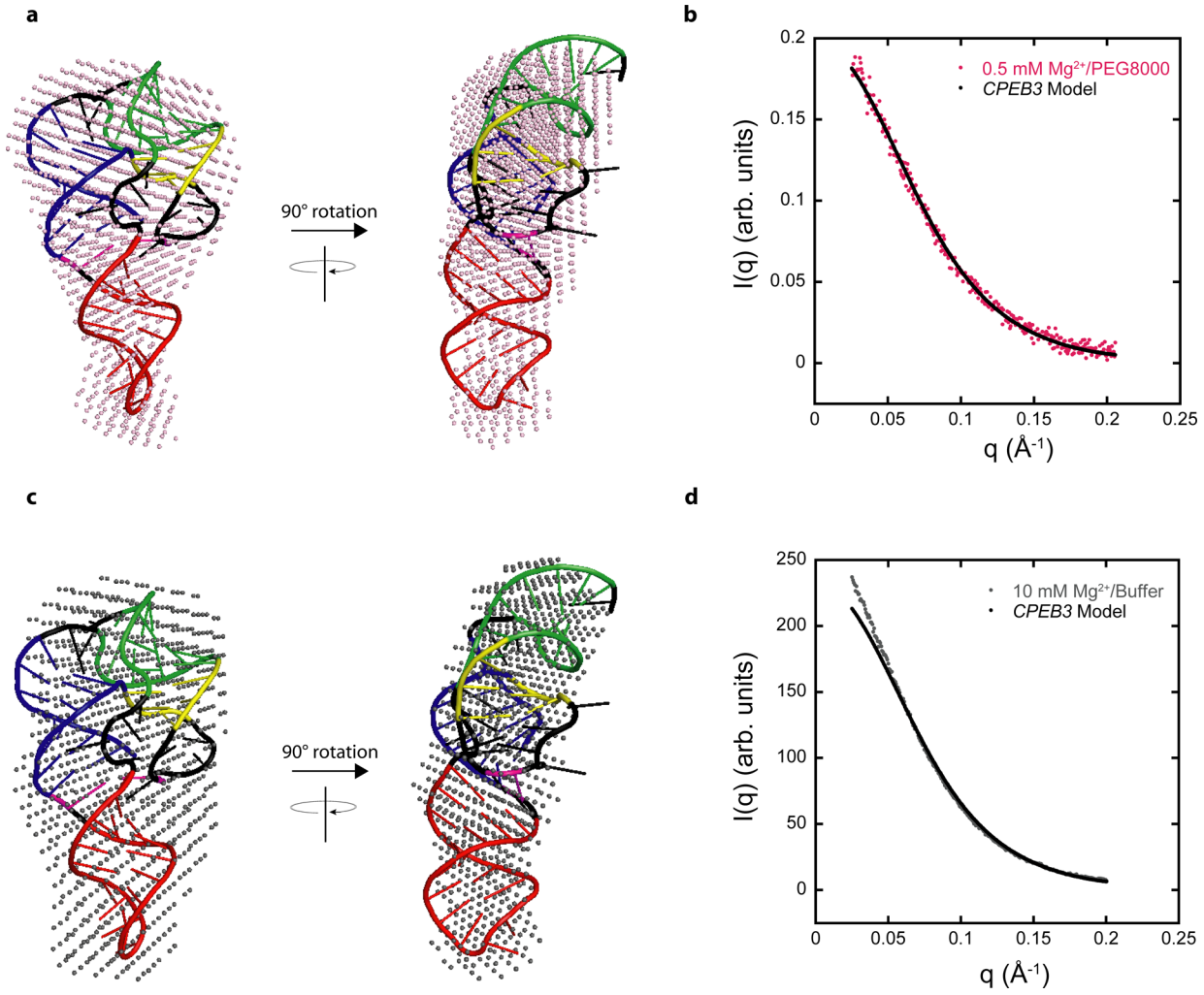

Figure 7. Model of the *CPEB3* ribozyme that agrees well with SAXS data. (a and c) SAXS reconstructions in (a) 0.5 mM Mg^{2+} and 20% PEG8000 (pink spheres) and (c) 10 mM Mg^{2+} without an additive (gray spheres) superimposed on the same *CPEB3* ribozyme model. The *CPEB3* ribozyme model was constructed from the HDV ribozyme crystal structure and color-coded according to the secondary structure in Figure 1. (b and d) Experimental scattering data for the *CPEB3* ribozyme in (b) 0.5 mM Mg^{2+} and 20% PEG8000 and (d) 10 mM Mg^{2+} without an additive plotted with the calculated scattering data from the native-state model. The calculated scattering profile for the *CPEB3* model was generated using the FoXS server.[36,37]

downward at high q values, indicating that the RNAs are folded. The peak shift for the PEG200 Kratky curve is to the right and slightly more elevated, which indicates that the RNA is less compact than that in buffer and PEG8000, consistent with the R_g and D_{max} values mentioned above.

SAXS Reconstructions Overlay Well with a Structural Model. Shape reconstruction was performed by running 10 independent DAMMIF calculations on the GNOM data.[38] The individual outputs were averaged to provide a single consensus reconstruction using DAMAVER.[39] From the consensus reconstruction, we calculated an excluded volume. The excluded volumes in 0.5 mM Mg^{2+} and buffer only, 20% PEG200, and 20% PEG8000 were 44555, 45570, and 40544 $Å^3$, respectively (Table 1). Clearly, the excluded volume is minimal in 20% PEG8000, indicating that this condition leads to the most compact state of the ribozyme, consistent with the R_g and D_{max} analyses provided above. These conclusions are strengthened by consideration of the rmsd for superposing the various SAXS-generated envelopes with our model of the *CPEB3* cleaved state, which revealed a value of 2.6 Å for PEG8000, but 3.4 and 3.8 Å for buffer and PEG200, respectively.

In 10 mM Mg^{2+}, consensus reconstructions were employed to calculate an excluded volume in buffer alone and PEG8000. The excluded volumes were 41280 and 30877 $Å^3$ in buffer alone and PEG8000, respectively. The excluded volume of the RNA in buffer alone agrees well with the excluded volume in 0.5 mM Mg^{2+} and PEG8000. The smaller excluded volume for the RNA in 10 mM Mg^{2+} and PEG8000 compared to that in 10 mM Mg^{2+} in buffer alone indicates that the crowding agent leads to further compaction, consistent with the R_g and D_{max} values listed above. On the basis of the observations described above, we focused superposition of the reconstruction and model on the data for 0.5 mM Mg^{2+} and PEG8000 and data for 10 mM Mg^{2+} and buffer alone.

Superpositions of the consensus reconstructions in 0.5 mM Mg^{2+} and 20% PEG8000 and in 10 mM Mg^{2+} and buffer alone with the model of the *CPEB3* ribozyme were achieved using SUPCOMB20.[40] The envelope reconstructions have low MNSD values of 0.33 and 0.65 in 0.5 mM Mg^{2+} and 20% PEG8000 and in 10 mM Mg^{2+} and buffer alone, respectively

dx.doi.org/10.1021/bi400816s | *Biochemistry* 2013, 52, 8187−8197

(Figure 7a,c). The envelope reconstruction for both sets of data has the same general shape as the native-state model and encompasses nearly the entire model (Figure 7a,c). The native-state model fits well throughout all portions of the reconstruction without excessive empty spaces, which supports the actual RNA folding in a fashion similar to that of our model. This conclusion is strengthened by the excellent agreement of the calculated scattering curve generated from the model and the experimental scattering curves, although there is slight deviation for the data in 10 mM Mg^{2+} and buffer alone (Figure 7b,d). In addition, we calculated R_g and D_{max} values of 20.4 and 73.8 Å, respectively, from the calculated scattering curve of the model, and these values are in excellent agreement with the R_g and D_{max} values of 21.8 and 75 Å, respectively, from the GNOM analysis in 0.5 mM Mg^{2+} and PEG8000 and R_g and D_{max} values of 22.6 and 75 Å, respectively, from the GNOM analysis in 10 mM Mg^{2+} and buffer alone. These results further support the conclusion that the RNA has an almost identical shape and compactness in 10 mM Mg^{2+} buffer alone as in 0.5 mM Mg^{2+} supplemented with a crowding agent, with slightly greater compactness at the lower Mg^{2+} concentrations with a crowding agent. These results strongly support the conclusion that activity facilitation of the ribozyme by crowding agents comes from increased compactness.

DISCUSSION

The majority of the studies of the structure and function in the RNA literature have been conducted at ≥5−10 mM Mg^{2+} or 1 M Na^+. This is because such ionic conditions tend to promote RNA folding and populate the native and functional state of a functional nucleic acid. Such behavior is of great utility for binding and enzymatic studies in riboswitches and ribozymes, and for nuclear magnetic resonance and X-ray crystallographic structural studies. Conditions in the cell are much different, however.

Concentrations of free magnesium ions in a eukaryotic cell are estimated to be only 0.2−1 mM,[42−45] concentrations that lead to much less robust RNA folding.[55,56] At the same time, cells are extremely crowded because of biopolymers and solutes such as NTPs and metabolites. The extent to which these additives influence RNA folding and function is an important one to address. In this study, we found that crowders and cosolutes facilitate ribozyme activity, up to ∼10-fold, but only in the presence of biological magnesium concentrations and denaturants. Indeed, we found that the molecular basis for the effect of the high-molecular weight crowder PEG8000 is compaction of the RNA, as demonstrated by R_g, D_{max}, and excluded volume values that are lower than those in buffer alone, as well as an overlay of a native-state model of the *CPEB3* ribozyme and averaged SAXS reconstructions. A key result is that biological Mg^{2+} and crowders give rise to SAXS profiles nearly identical to those under standard literature conditions of 10 mM Mg^{2+}. While others have shown that specific ligands can offer such compaction, such as in the case of riboswitches,[57,58] the effect in our study appears to be due to general, less specific effects.

The importance of compaction is emphasized by observation that reactivity of the C-2A fast-reacting version of the ribozyme, which has to populate the same native state, is also facilitated by PEG8000 and Dextran10. It thus appears that the basis for a high-molecular weight crowder facilitating ribozyme function is related to its ability to compact the RNA into the native state. Scheme 1 summarizes these data. Shown are three states, M, I, and N, for misfolded, intermediate, and native states, respectively. The wild-type ribozyme can populate the Alt P1 pairing, in which upstream nucleotides mispair with the P1.1-forming G37; this state is depicted as M. The C-2A mutant destabilizes Alt P1, allowing the native P1 to form, depicted as I because further additive stimulates this state to the true N state.[23] Given that PEG8000 compacts the cleaved state and favors reactivity, we depict this as populating the native state, which is common to both WT and C-2A RNAs.

Moreover, this relationship offers an explanation of why crowding does not facilitate reactivity in the background of strongly folding 10 mM Mg^{2+} conditions, as the RNA is already well folded in this case. Consistent with this notion, if the RNA is moderately denatured in 2.5 M urea, these same additives stimulate ribozyme function in the presence of 10 mM Mg^{2+}. Moreover, this facilitation can occur both at the start of the reaction and partially through the progress of the reaction, suggesting that crowding can act both as a protectant and as a renaturant.

Notably, 10 mM Mg^{2+} conditions lead to a number of problems with folding of the *CPEB3* ribozyme at SAXS concentrations of RNA. In particular, the ribozyme aggregates, as revealed by both native gels and the SAXS analyses. Aggregation was overcome in two ways in our study. One method we used was to isolate a monomeric fraction of the RNA by SEC just prior to SAXS analysis, and a second way was through the addition of the crowding agent to the 10 mM Mg^{2+} sample, which also provided monomeric SAXS data. We do note that Mg^{2+} has been reported to drive aggregation of other RNA molecules according to SAXS studies.[59]

PEG200 stimulates the ribozyme reaction to approximately the same extent as PEG8000; however, the origin of the PEG200 effect is less clear. Our data clearly show that PEG200 operates by a mechanism different from that of PEG8000. In particular, R_g, D_{max}, and excluded volume values provide no evidence that PEG200 leads to compaction of the RNA and in fact suggest that PEG200 may lead to a modest expansion of the RNA, a conclusion that is consistent with studies by Record and co-workers who indicated that PEG200 does not crowd the solution.[41] In fact, this same study provided evidence that PEG200 directly interacts with DNA nucleotides,[41] while other studies showed that PEG200 destabilizes RNA and DNA secondary structure.[5] How such features drive ribozyme catalysis is not clear at present, but there has been evidence that PEG200 lowers the dielectric of the solution, which could enhance metal binding,[21] although PEG in general does not appear to alter the activity of Mg^{2+}.

The fold-effects of additives on ribozyme cleavage rate found in our study are similar in magnitude to those found for seminal studies on the hammerhead ribozyme by Nakano and co-workers, who observed that 20% PEG8000 afforded an ∼10-fold stimulation of the rate in 3 mM Mg^{2+}.[5] However, it is important to point out several important ways in which our study differs from theirs. First, we studied a human ribozyme under conditions relevant to a eukaryotic cell. Second, we examined the effect of chemical denaturants and rescue by additives. Third, and most importantly, we provided a structural basis for the effects through our SAXS studies. These studies demonstrate compaction of the RNA by the additives at biological Mg^{2+} concentrations. Moreover, through comparison to a fast-reacting variant of the *CPEB3* ribozyme, we provide evidence that our effects operate through favoring the fold of the native state.

Overall, cellular-like conditions of low ionic strength and crowding clearly influence RNA folding and thus the optimal activity of functional RNAs. It may be the case that crowders will stimulate the function of many ribozymes and riboswitches and that at least part of the mechanism will involve favoring a native compact state. Furthermore, such effects are expected to be enhanced for RNAs that start off in less compact states such as those present in biological magnesium concentrations. It will be of great interest to test the extent to which cellular conditions alter the folding and function of other RNAs.

■ ASSOCIATED CONTENT

Supporting Information

Additional figures for kinetic experiments, SAXS experiments, vapor-pressure osmometry, and native gel electrophoresis. Descriptions of vapor-pressure osmometry and native gel electrophoresis. This material is available free of charge via the Internet at http://pubs.acs.org.

■ AUTHOR INFORMATION

Corresponding Author

*E-mail: pcb5@psu.edu. Telephone: (814) 863-3812.

Funding

This work is based upon research conducted at the Cornell High Energy Synchrotron Source (CHESS), which is supported by National Science Foundation Grant DMR-0936384 and National Institute of General Medical Sciences Grant GM-103485. The SIBYLS beamline is supported by National Institute of General Medical Sciences project MINOS (Macromolecular INsights Optimized by Scattering) and by U.S. Department of Energy program Integrated Diffraction Analysis Technologies Grant DEAC02-05CH11231. This work was supported by NASA Grant NNX13AI01G.

Notes

The authors declare no competing financial interest.

■ ACKNOWLEDGMENTS

We thank The Penn State University macromolecular X-ray crystallography core facility for the use of the dynamic light scattering instrument and Richard Gillilan for help with acquiring SAXS data. We also thank Lois Pollack, Durga Chadalavada, and Josh Blose for assistance.

■ ABBREVIATIONS

CPEB3 ribozyme, cytoplasmic polyadenylation element-binding protein 3 HDV-like ribozyme; C-2A, variant of the *CPEB3* ribozyme in which the C at upstream −2 position is mutated to an A; Dextran10, dextran with an average molecular weight of 10 kDa; HDV, hepatitis delta virus; PEG200, polyethylene glycol with an average molecular weight of 200 Da; PEG8000, polyethylene glycol with an average molecular weight of 8 kDa; rmsd, root-mean-square deviation; SAXS, small-angle X-ray scattering; SEC, size-exclusion chromatography; VPO, vapor-pressure osmometry.

■ ADDITIONAL NOTE

[a]These effects are unlikely to be due to viscosity changes. The ribozyme reactions studied herein are single-turnover reactions and so do not depend on substrate association or product release. Moreover, the lack of an effect of additives on the reaction at 10 mM Mg^{2+}, where they change the viscosity of the solution by similar amounts as at lower Mg^{2+} concentrations, argues that viscosity changes play at most a minor role in the rate enhancements.

■ REFERENCES

(1) Strulson, C. A., Molden, R. C., Keating, C. D., and Bevilacqua, P. C. (2012) RNA catalysis through compartmentalization. *Nat. Chem. 4*, 941−946.

(2) Minton, A. P. (2001) The influence of macromolecular crowding and macromolecular confinement on biochemical reactions in physiological media. *J. Biol. Chem. 276*, 10577−10580.

(3) Ellis, R. J. (2001) Macromolecular crowding: Obvious but underappreciated. *Trends Biochem. Sci. 26*, 597−604.

(4) Kilburn, D., Roh, J. H., Guo, L., Briber, R. M., and Woodson, S. A. (2010) Molecular crowding stabilizes folded RNA structure by the excluded volume effect. *J. Am. Chem. Soc. 132*, 8690−8696.

(5) Nakano, S., Karimata, H. T., Kitagawa, Y., and Sugimoto, N. (2009) Facilitation of RNA enzyme activity in the molecular crowding media of cosolutes. *J. Am. Chem. Soc. 131*, 16881−16888.

(6) Karimata, H., Nakano, S., and Sugimoto, N. (2006) The roles of cosolutes on the hammerhead ribozyme activity. *Nucleic Acids Symp. Ser. 50*, 81−82.

(7) Kassel, K. M., Au, D. R., Higgins, M. J., Hines, M., and Graves, L. M. (2010) Regulation of human cytidine triphosphate synthetase 2 by phosphorylation. *J. Biol. Chem. 285*, 33727−33736.

(8) Bergström, J., Fürst, P., Norée, L. O., and Vinnars, E. (1974) Intracellular free amino acid concentration in human muscle tissue. *J. Appl. Physiol. 36*, 693−697.

(9) Bar-Even, A., Noor, E., Flamholz, A., Buescher, J. M., and Milo, R. (2011) Hydrophobicity and charge shape cellular metabolite concentrations. *PLoS Comput. Biol. 7*, e1002166.

(10) Zhou, H. X., Rivas, G., and Minton, A. P. (2008) Macromolecular crowding and confinement: Biochemical, biophysical, and potential physiological consequences. *Annu. Rev. Biophys. 37*, 375−397.

(11) Knowles, D. B., Lacroix, A. S., Deines, N. F., Shkel, I., and Record, M. T., Jr. (2011) Separation of preferential interaction and excluded volume effects on DNA duplex and hairpin stability. *Proc. Natl. Acad. Sci. U.S.A. 108*, 12699−12704.

(12) Guinn, E. J., Schwinefus, J. J., Cha, H. K., McDevitt, J. L., Merker, W. E., Ritzer, R., Muth, G. W., Engelsgjerd, S. W., Mangold, K. E., Thompson, P. J., Kerins, M. J., and Record, M. T. (2013) Quantifying functional group interactions that determine urea effects on nucleic acid helix formation. *J. Am. Chem. Soc. 135*, 5828−5838.

(13) Nakano, S., Hirayama, H., Miyoshi, D., and Sugimoto, N. (2012) Dimerization of nucleic acid hairpins in the conditions caused by neutral cosolutes. *J. Phys. Chem. B 116*, 7406−7415.

(14) Kim, Y. C., Best, R. B., and Mittal, J. (2010) Macromolecular crowding effects on protein-protein binding affinity and specificity. *J. Chem. Phys. 133*, 205101.

(15) Wang, Y., Sarkar, M., Smith, A. E., Krois, A. S., and Pielak, G. J. (2012) Macromolecular crowding and protein stability. *J. Am. Chem. Soc. 134*, 16614−16618.

(16) Jiang, M., and Guo, Z. (2007) Effects of macromolecular crowding on the intrinsic catalytic efficiency and structure of enterobactin-specific isochorismate synthase. *J. Am. Chem. Soc. 129*, 730−731.

(17) Tokuriki, N., Kinjo, M., Negi, S., Hoshino, M., Goto, Y., Urabe, I., and Yomo, T. (2004) Protein folding by the effects of macromolecular crowding. *Protein Sci. 13*, 125−133.

(18) Nashimoto, M. (2000) Correct folding of a ribozyme induced by nonspecific macromolecules. *Eur. J. Biochem. 267*, 2738−2745.

(19) Nakano, S., Kitagawa, Y., Karimata, H. T., and Sugimoto, N. (2008) Molecular crowding effect on metal ion binding properties of the hammerhead ribozyme. *Nucleic Acids Symp. Ser. 52*, 519−520.

(20) Lambert, D., and Draper, D. E. (2007) Effects of osmolytes on RNA secondary and tertiary structure stabilities and RNA-Mg^{2+} interactions. *J. Mol. Biol. 370*, 993−1005.

(21) Nakano, S., Hirayama, H., Miyoshi, D., and Sugimoto, N. (2012) Dimerization of nucleic acid hairpins in the conditions caused by neutral cosolutes. *J. Phys. Chem. B 116*, 7406−7415.

(22) Salehi-Ashtiani, K., Lupták, A., Litovchick, A., and Szostak, J. W. (2006) A genomewide search for ribozymes reveals an HDV-like sequence in the human CPEB3 gene. *Science 313*, 1788−1792.
(23) Chadalavada, D. M., Gratton, E. A., and Bevilacqua, P. C. (2010) The human HDV-like CPEB3 ribozyme is intrinsically fast-reacting. *Biochemistry 49*, 5321−5330.
(24) Emsley, P., and Cowtan, K. (2004) Coot: Model-building tools for molecular graphics. *Acta Crystallogr. D60*, 2126−2132.
(25) Vanegas, P. L., Hudson, G. A., Davis, A. R., Kelly, S. C., Kirkpatrick, C. C., and Znosko, B. M. (2012) RNA CoSSMos: Characterization of Secondary Structure Motifs: A searchable database of secondary structure motifs in RNA three-dimensional structures. *Nucleic Acids Res. 40*, D439−D444.
(26) Krieger, E., Joo, K., Lee, J., Lee, J., Raman, S., Thompson, J., Tyka, M., Baker, D., and Karplus, K. (2009) Improving physical realism, stereochemistry, and side-chain accuracy in homology modeling: Four approaches that performed well in CASP8. *Proteins: Struct., Funct., Bioinf. 77*, 114−122.
(27) Nielsen, S. S., Toft, K. N., Snakenborg, D., Jeppesen, M. G., Jacobsen, J. K., Vestergaard, B., Kutter, J. P., and Arleth, L. (2009) BioXTAS RAW, a software program for high-throughput automated small-angle X-ray scattering data reduction and preliminary analysis. *J. Appl. Crystallogr. 42*, 959−964.
(28) Meisburger, S. P., Warkentin, M., Chen, H., Hopkins, J. B., Gillilan, R. E., Pollack, L., and Thorne, R. E. (2013) Breaking the radiation damage limit with cryo-SAXS. *Biophys. J. 104*, 227−236.
(29) Classen, S., Hura, G. L., Holton, J. M., Rambo, R. P., Rodic, I., McGuire, P. J., Dyer, K., Hammel, M., Meigs, G., Frankel, K. A., and Tainer, J. A. (2013) Implementation and performance of SIBYLS: A dual endstation small-angle X-ray scattering and macromolecular crystallography beamline at the Advanced Light Source. *J. Appl. Crystallogr. 46*, 1−13.
(30) Rambo, R. P., and Tainer, J. A. (2010) Improving small-angle X-ray scattering data for structural analyses of the RNA world. *RNA 16*, 638−646.
(31) Guinier, A., and Fournet, G. (1955) *Small-angle scattering of X-rays*, Wiley, New York.
(32) Semenyuk, A. V., and Svergun, D. I. (1991) GNOM: A program package for small-angle scattering data processing. *J. Appl. Crystallogr. 24*, 537−540.
(33) Svergun, D. I. (1992) Determination of the regularization parameter in indirect-transform methods using perceptual criteria. *J. Appl. Crystallogr. 25*, 495−503.
(34) Hura, G. L., Menon, A. L., Hammel, M., Rambo, R. P., Poole, F. L., II, Tsutakawa, S. E., Jenney, F. E., Jr., Classen, S., Frankle, K. A., Hopkins, R. C., Yang, S. J., Scott, J. W., Dillard, B. D., Adams, M. W., and Tainer, J. A. (2009) Robust, high-throughput solution structural analyses by small angle X-ray scattering (SAXS). *Nat. Methods 6*, 606−612.
(35) Durand, D., Vives, C., Cannella, D., Perez, J., Pebay-Peyroula, E., Vachette, P., and Fieschi, F. (2010) NADPH oxidase activator p67(phox) behaves in solution as a multidomain protein with semi-flexible linkers. *J. Struct. Biol. 169*, 45−53.
(36) Schneidman-Duhovny, D., Hammel, M., and Sali, A. (2010) FoXS: A web server for rapid computation and fitting of SAXS profiles. *Nucleic Acids Res. 38*, W540−W544.
(37) Schneidman-Duhovny, D., Hammel, M., Tainer, J. A., and Sali, A. (2013) Accurate SAXS profile computation and its assessment by contrast variation experiments. *Biophys. J. 105*, 962−974.
(38) Franke, D., and Svergun, D. I. (2009) DAMMIF, a program for rapid *ab-initio* shape determination in small-angle scattering. *J. Appl. Crystallogr. 42*, 342−346.
(39) Volkov, V. V., and Svergun, D. I. (2003) Uniqueness of *ab initio* shape determination in small-angle scattering. *J. Appl. Crystallogr. 36*, 860−864.
(40) Kozin, M. B., and Svergun, D. I. (2001) Automated matching of high- and low-resolution structural models. *J. Appl. Crystallogr. 34*, 33−41.
(41) Knowles, D. B., LaCroix, A. S., Deines, N. F., Shkel, I., and Record, M. T. (2011) Separation of preferential interaction and excluded volume effects on DNA duplex and hairpin stability. *Proc. Natl. Acad. Sci. U.S.A. 108*, 12699−12704.
(42) London, R. E. (1991) Methods for measurement of intracellular magnesium: NMR and fluorescence. *Annu. Rev. Physiol. 53*, 241−258.
(43) Grubbs, R. D. (2002) Intracellular magnesium and magnesium buffering. *BioMetals 15*, 251−259.
(44) Alberts, B., Bray, D., Lewis, J., Raff, M., Roberts, K., and Watson, J. D. (1994) *Molecular biology of the cell*, 3rd ed., Garland Science, New York.
(45) Feig, A. L., and Uhlenbeck, O. C. (1999) The role of metal ions in RNA biochemistry. In *The RNA World*, 2nd ed. Gesteland, R. F., Cech, T. R., Atkins, J. F., Eds.; Cold Spring Harbor Laboratory Press, Plainview, NY; pp 287−319.
(46) Chen, J., Ganguly, A., Miswan, Z., Hammes-Schiffer, S., Bevilacqua, P. C., and Golden, B. L. (2013) Identification of the catalytic Mg^{2+} ion in the hepatitis delta virus ribozyme. *Biochemistry 52*, 557−567.
(47) Denesyuk, N. A., and Thirumalai, D. (2011) Crowding promotes the switch from hairpin to pseudoknot conformation in human telomerase RNA. *J. Am. Chem. Soc. 133*, 11858−11861.
(48) Yancey, P. H., Clark, M. E., Hand, S. C., Bowlus, R. D., and Somero, G., N. (1982) Living with water stress: Evolution of osmolyte systems. *Science 217*, 1214−1222.
(49) Rösgen, J., Pettitt, B. M., and Bolen, D. W. (2005) Protein folding, stability, and solvation structure in osmolyte solutions. *Biophys. J. 89*, 2988−2997.
(50) Shelton, V. M., Sosnick, T. R., and Pan, T. (1999) Applicability of urea in the thermodynamic analysis of secondary and tertiary RNA folding. *Biochemistry 38*, 16831−16839.
(51) Priyakumar, U. D., Hyeon, C., Thirumalai, D., and MacKerell, A. D. (2009) Urea destabilizes RNA by forming stacking interactions and multiple hydrogen bonds with nucleic acid bases. *J. Am. Chem. Soc. 131*, 17759−17761.
(52) Ferre-D'Amare, A. R., Zhou, K., and Doudna, J. A. (1998) Crystal structure of a hepatitis delta virus ribozyme. *Nature 395*, 567−574.
(53) Russell, R., Zhuang, X., Babcock, H. P., Millett, I. S., Doniach, S., Chu, S., and Herschlag, D. (2002) Exploring the folding landscape of a structured RNA. *Proc. Natl. Acad. Sci. U.S.A. 99*, 155−160.
(54) Lipfert, J., Herschlag, D., and Doniach, S. (2009) Riboswitch conformations revealed by small-angle X-ray scattering. *Methods Mol. Biol. 540*, 141−159.
(55) Fang, X., Littrell, K., Yang, X. J., Henderson, S. J., Siefert, S., Thiyagarajan, P., Pan, T., and Sosnick, T. R. (2000) Mg^{2+}-dependent compaction and folding of yeast $tRNA^{Phe}$ and the catalytic domain of the *B. subtilis* RNase P RNA determined by small-angle X-ray scattering. *Biochemistry 39*, 11107−11113.
(56) Misra, V. K., Shiman, R., and Draper, D. E. (2003) A thermodynamic framework for the magnesium-dependent folding of RNA. *Biopolymers 69*, 118−136.
(57) Lipfert, J., Das, R., Chu, V. B., Kudaravalli, M., Boyd, N., Herschlag, D., and Doniach, S. (2007) Structural transitions and thermodynamics of a glycine-dependent riboswitch from *Vibrio cholerae*. *J. Mol. Biol. 365*, 1393−1406.
(58) Chen, B., Zuo, X., Wang, Y. X., and Dayie, T. K. (2012) Multiple conformations of SAM-II riboswitch detected with SAXS and NMR spectroscopy. *Nucleic Acids Res. 40*, 3117−3130.
(59) Schlatterer, J. C., Kwok, L. W., Lamb, J. S., Park, H. Y., Andresen, K., Brenowitz, M., and Pollack, L. (2008) Hinge stiffness is a barrier to RNA folding. *J. Mol. Biol. 379*, 859−870.